Measurement of effective dielectronic recombination rates for Fe IX, X, and XI

R. L. Brooks, R. U. Datla, A. D. Krumbein, and Hans R. Griem

Department of Physics and Astronomy, University of Maryland, College Park, Maryland 20742
(Received 3 October 1979)

Effective rate coefficients for dielectronic recombination of Fe-IX, -X, and -XI ions at electron densities in the range of 3×10^{16} cm^{-3} and electron temperatures up to 220 eV, were deduced from the time histories of emission lines in a small θ-pinch plasma. The iron impurity in the hydrogen plasma was introduced by a laser puffing method. The intensities of lines from these ionization stages were measured as functions of time and interpreted by means of a time-dependent corona ionization-recombination model. A one-dimensional computer code, which takes into account the radial variations of T_e and n_e, was used for the simulation of time histories. The effective rate coefficients were found to be equal to or smaller than currently accepted theoretical values for low-density plasmas.

I. INTRODUCTION

The lifetime of the various ionic stages of heavy impurity ions in high-temperature hydrogen or deuterium and tritium plasmas is an important quantity in astrophysics and in controlled-fusion research. The basic processes governing the ionic lifetimes are electron-impact ionization and the various recombination processes—radiative, dielectronic, and three body—or charge exchange, whose relative importance is determined by the plasma conditions. In many high-temperature plasmas of interest, ranging from the solar corona to tokamak experiments, dielectronic recombination dominates the other recombination processes and strongly shifts the ionization-recombination balance in favor of lower ionization stages.

To date, measurements of this important rate process have been performed only for the case of Fe ions (Fe IX, X, and XI), using a θ-pinch apparatus,[1] and for Mo ions occurring in tokamak plasmas.[2] Both of these measurements involve the time histories of resonance lines, whose intensities reflect the varying populations of the respective ground states due to ionization and recombination processes. In other words, dielectronic recombination is not determined via the corresponding satellites which would mostly not be resolved. Rather, it is assumed that the contribution of the unresolved satellites is negligibly small.

The purpose of this article is to present in detail the experimental observations that were briefly communicated in Ref. 1, together with revised values for the effective recombination-rate coefficients arrived at by using improved computer simulations of the impurity line emission.

In Sec. II, we describe the experiment and in Secs. III and IV the computer modeling, i.e.. the simulated time histories of emission lines of iron

ions obtained by using effective ionization- and recombination-rate coefficients that best match the experimental time histories. In this process the ionization rates presented in Ref. 1 remained unchanged; however, improved values for effective recombination rates were obtained.

II. THE EXPERIMENT

A low-energy θ-pinch device was used as a plasma source for this experiment. It, and the diagnostic apparatus, are essentially the same as those used in the previously reported ionization-rate measurements.[3,4] The overall experimental arrangement is shown in Fig. 1.

Two major improvements were made in the experimental technique. First, the iron-line emission was measured side-on by connecting the grazing-incidence monochromator through an extension tube to a 1-cm hole drilled into the side of the quartz discharge tube. This makes the line of sight a diameter in the midplane of the tube in which the Thomson-scattering measurements for the determination of electron temperature and density are also made. These latter measurements were taken at four points along the radius of the plasma. The second improvement was in the method of impurity introduction into the hydrogen plasma. A laser puffing method was used as described in Ref. 1. (The method was first used by E. S. Marmar *et al.*[5] to study impurity transport in tokamaks.)

Peak electron temperature and density achieved in the θ-pinch were varied in two ways: by changing the initial filling pressure of hydrogen gas, and by changing the voltage to which the main bank was charged before firing. Lowering the fill pressure of hydrogen would typically decrease the density and increase the peak temperature of the plas-
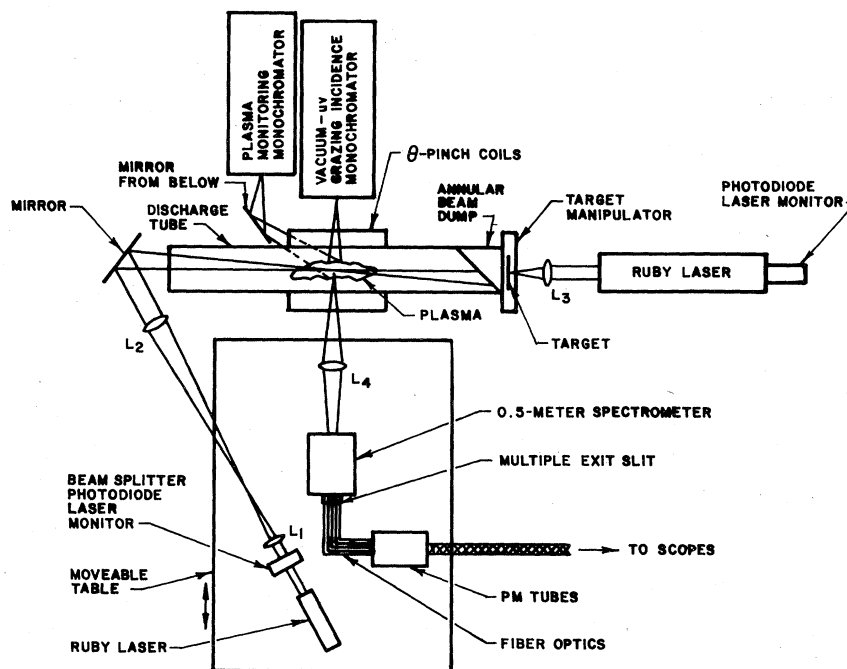
FIG. 1. The experimental arrangement.

ma produced. Lowering the main bank voltage de-creased both peak density and temperature. Three plasma conditions were studied for this work, two of which used full main bank voltage of 38 kV with initial H_2 pressures of 10 mTorr and 45 mTorr, respectively, while the third used only 31 kV on the main bank and a 38-mTorr fill of H_2. In each case the hydrogen-gas equilibrium pressure was main-tained by regulating the constant H_2 flow through the tube with a needle valve and a small-diameter pumping port.

For each plasma condition at least three, and usually more, lines were observed for each of the higher ionization stages of iron. Table I lists the lines of Fe VIII–Fe XII which were observed with the 2-m grazing-incidence monochromator with an exit slit width corresponding to 0.4 Å. In each plasma condition, time histories of all lines of a given ionization stage were the same except for the $3p^5 d(^1P_1) - 3p^6(^1S_0)$ transition of Fe IX at 171.1 Å in plasma cases II and III. The time history of this line was not used in our considerations and the possibility of blending with an unknown impurity line could not be ruled out. The experimentally observed time histories, averaged over shots and lines, are shown in Figs. 2–4. The plateau re-gions in the time histories of Fe IX and Fe X in cases III and II are evident as are the fast oscilla-

TABLE I. Observed lines and transitions for Fe VIII–XII.

| Transition	λ (Å)	Transition	λ (Å)
Fe VIII		**Fe IX**	
$3p^6 4f\ ^2F - 3p^6 3d\ ^2D$	131.1	$3p^5 4s\ ^3P_1 - 3p^6\ ^1S_0$	105.2
$3p^5 3d^2 - 3p^6 3d$:		$3p^5 4f - 3p^5 3d$:	
$(^3P)^2 P_{3/2} - ^2D_{5/2}$	168.6	$^3D - ^3P$	111.9
$(^3P)^2 P_{1/2} - ^2D_{3/2}$	168.9	$^3G - ^3F$	114
$(^3F)^2 F_{7/2} - ^2D_{5/2}$	185.2	$3p^5 3d - 3p^6$	
$(^3F)^2 F_{5/2} - ^2D_{3/2}$	186.6	$^1P_1 - ^1S_0$	171.1
Fe X		$^3D_1 - ^1S_0$	217.1
$3p^4 4s - 3p^5$:		**Fe XI**	
$^2D_{5/2} - ^2P_{3/2}$	94.0	$3p^3 3d\ ^1F - 3p^4\ ^1D$	179.8
$^2P_{3/2} - ^2P_{3/2}$	96.1	$3p^3 3d\ ^3P - 3p^4\ ^3P$	188.3
$3p^4 3d\ ^2D - 3p^5\ ^2P$	174.6	$3s 3p^5 - 3s^2 3p^4$:	
$3s 3p^6\ ^2S - 3p^5\ ^2P$	365.6	$^1P_1 - ^1D_2$	308.6
Fe XII		$^3P_2 - ^3P_2$	352.7
$3p^2 3d - 3p^3$:			
$(^1D)^2 F_{7/2} - ^2D_{5/2}$	186.9		
$(^3P)^4 P_{5/2} - ^4S_{3/2}$	195.1		
$3s 3p^4\ ^4P - 3s^2 3p^3\ ^4S$	352.1		
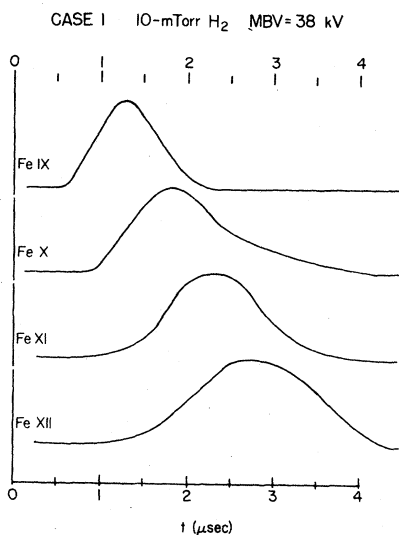
FIG. 2. Observed iron-line time histories—case I. (MBV on this figure and the following Figs. 3–9 refers to main bank voltage.)
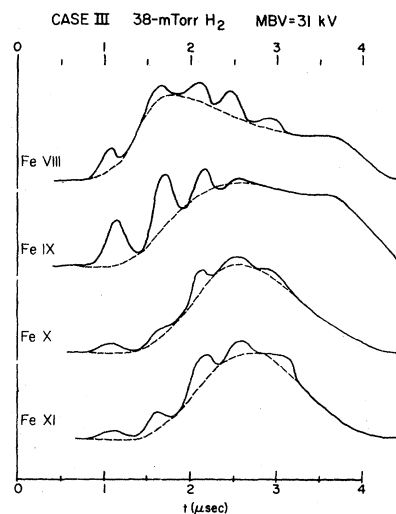

FIG. 4. Observed iron-line time histories—case III. Dashed curves are smoothed time histories.

tions occurring for all the time histories for these two cases. These oscillations are in phase with the electron density oscillations observed in the Thomson-scattering data. Smoothed time histories are shown by the dashed curves in Figs. 3 and 4.

The volume-averaged electron densities and temperatures determined from the laser-scattering measurements are shown in Figs. 5 and 6. The oscillations observed in cases II and III are probably radial "breathing" modes in which the
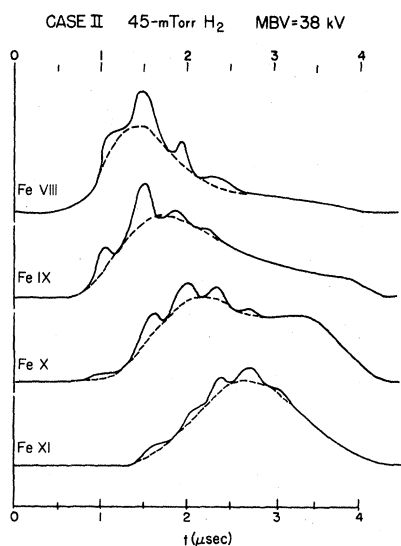

FIG. 3. Observed iron-line time histories—case II. Dashed curves are smoothed time histories.
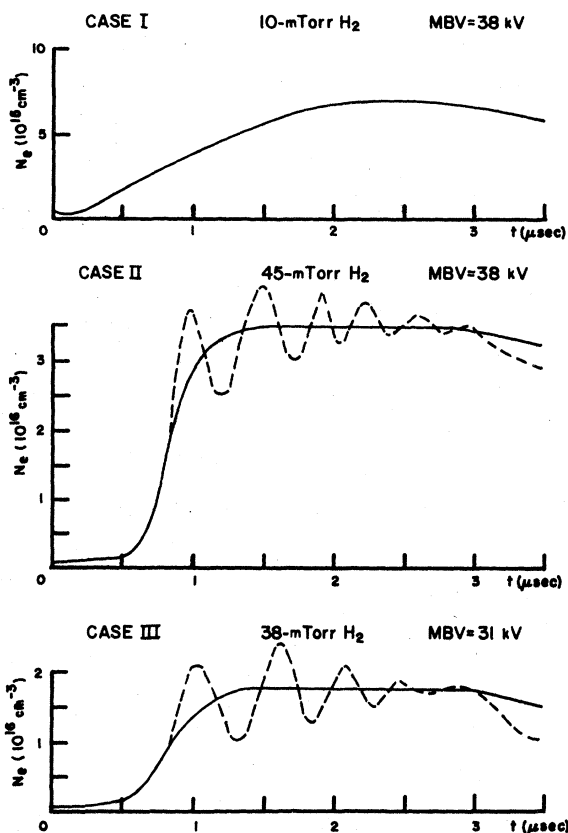

FIG. 5. Radially averaged electron density (solid curves are smoothed, dashed curves are as observed).
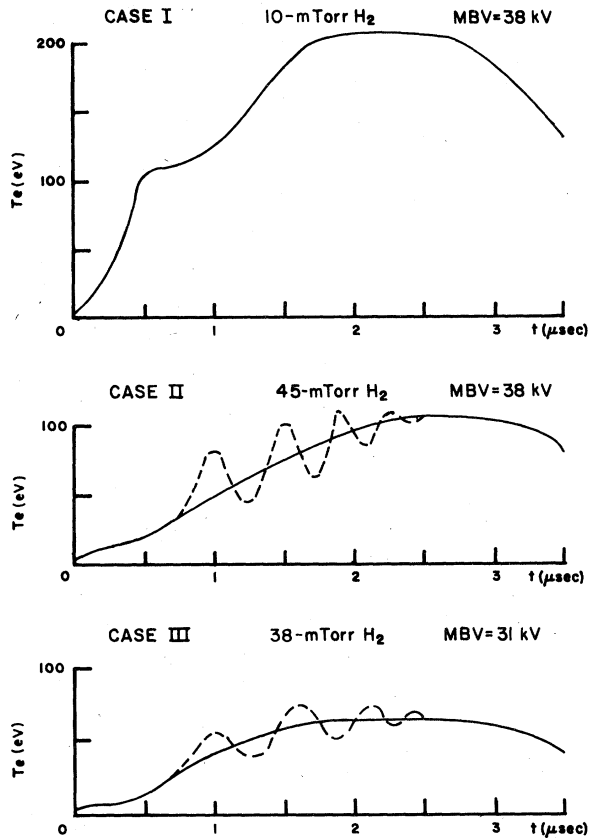
FIG. 6. Radially averaged electron temperature
(solid curves are smoothed, dashed curves are as ob-
served).

imploding plasma column overshoots its equilib-
rium radius as a near-sinusoidal function of time.
The period and amplitude of these oscillations are
consistent with plasma simulations performed by
us using the hybrid code (fluid electrons, Vlasov
ions) of Sgro and Nielson.[6] However, phases of the
oscillations and actual values of measured and cal-
culated densities and temperatures differ, probably
because end losses are important in the experi-
ment. On the other hand, these calculations con-
firm that radiation losses associated with the in-
jected iron (~0.05%) are not important.

The smoothed average temperature and density
histories used in the first computer analysis[1] are
also shown in Figs. 5 and 6. Confidence in the re-
sults obtained by neglecting the breathing-mode
oscillations must be based on comparisons with
the results of more extensive calculations which
include the oscillations. Such calculations were
made and are discussed with the computer-simu-
lation results.

III. COMPUTER SIMULATION OF IMPURITY LINE TIME HISTORIES

Since it is safe to assume that, for electron den-
sities usually encountered in magnetically confined
laboratory plasmas, radiative decay of excited
states is immediate and much more likely than
other decay processes, practically all ions will be
in their respective ground states.[3,4] The distribu-
tion of ions, N_z, of a given element over various
charge states is given by the set of coupled rate
equations

$$\frac{dN_z}{dt} = N_e[S_{z-1}N_{z-1} + \alpha_{z+1}N_{z+1} - (S_z + \alpha_z)N_z], \qquad (1)$$

where N_e is the electron density; S_z, the total ef-
fective rate coefficient for ionization; and α_z, the
total effective rate coefficient for recombination.
These coupled rate equations are solved numeri-
cally with the measured electron density and tem-
perature as input. To account for compression, a
term dN_e/dt should be added to Eq. (1). However,
this term was numerically insignificant in our
work.

The ionization-rate coefficient was calculated
using the semiempirical formula of Lotz and
Kunze[3,7]:

$$S(Z) = A(Z)\left[\left(\ln\frac{40 \times T_e}{E_i}\right)^3 + 40\right]$$

$$\times \frac{T_e^{1/2}}{E_i + 3T_e}e^{-E_i/T_e} \text{ cm}^3/\text{sec}, \qquad (2)$$

$$A(Z) = 7.5 \times 10^{-8}\frac{\eta_i}{E_i} \qquad (3)$$

which is given as input; E_i is the ionization energy
(eV); T_e, the electron temperature (eV); and η_i
the number of electrons in the ith subshell.

Of the three recombination processes mentioned
in the Introduction, only dielectronic recombina-
tion contributed significantly to the results. The
dielectronic recombination-rate coefficients cal-
culated by Jacobs et al.[8] were directly inputted in-
to the code. Radiative recombination was com-
puted using the formula due to Seaton,[9] but its con-
tribution was found to be quite small, and it was
not considered in the later calculations. Three-
body recombination, as calculated by a formula
due to Griem,[10] contributed even less to the time
histories and was, therefore, left out of all but the
preliminary calculations.

Once the time history of the ionic populations has
been determined, the time histories of their emis-
sion lines can be calculated using an expression
for the emission coefficient of an optically thin
allowed line whose upper level is populated mainly
by electron collisions from the ground state, viz.,

$$\epsilon_i = (h\nu/4\pi)N_e N_i X, \tag{4}$$

where N_i is the ground-state population of the ith ionization stage and X the excitation-rate coefficient from the ground state.

If N_e and X are known, one can calculate the time history of a line by knowing the time development of N_i. In the present work, N_e is known from Thomson scattering. We assume the effective-Gaunt-factor approximation for X because this approximation should give the correct temperature dependence, at least over the relatively small range of temperature studied here. X is then given by (in cm^3/sec)

$$X_{ij} = \frac{1.6 \times 10^{-5} f_{ij} \langle \bar{g} \rangle}{\Delta E (T_e)^{1/2}} e^{-\Delta E/T_e}, \tag{5}$$

where f_{ij} is the atomic oscillator strength; ΔE the transition energy, and $\langle \bar{g} \rangle$ the averaged Gaunt factor.

The approximate rate coefficients of ionization and recombination calculated by the methods just described may now be changed by variable factors, and the time histories of the lines can be recalculated until values which best match the experimental observations are obtained. By this process one can arrive at a set of effective ionization and recombination coefficients that best describe the system under study within, of course, the confines of the simulation procedure.

IV. RESULTS

Figure 7 shows a comparison between the time histories according to the computer code (solid curves) and the experimentally observed behavior (dashed curves) from Fig. 2, for case I. (In this and all subsequent graphs of the time history of the line intensities, the curves are normalized to the peak value of the intensity of each line.) In this high-temperature, low-density case, the theoretical predictions for recombination rates were always less than 15% of the corresponding ionization rates for the ions studied, and were not expected to significantly affect the line time histories. Note that the time histories are fairly symmetric in rise and decay, and peak at approximately equal intervals, the peak occurring at later times for higher ionization states. These are features found to be typical of a rapidly ionizing plasma in which recombination is small.

The computer calculations for case I bore out the expectation that recombination was negligible in this plasma condition. Simulations which included recombination of the magnitude predicted by Jacobs et al.[8] for low-density plasmas showed no significant difference from the time histories calculated without recombination. The computer
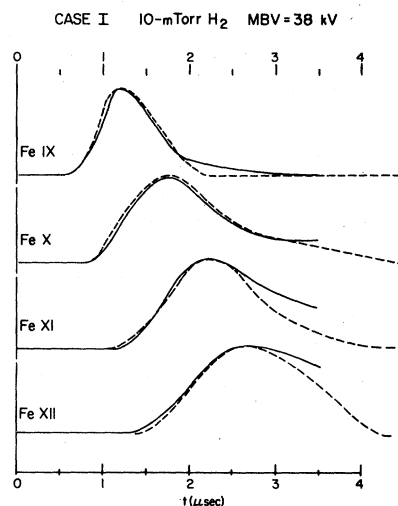

FIG. 7. Comparison of simulated (solid curves) and observed (dashed curves) time histories—case I.

simulation which generated the solid curves in Fig. 7 assumed recombination-rate coefficients as determined to fit cases II and III, but would not have been noticeably different had recombination been assumed several times larger, or been neglected entirely.

In contrast, as little as 15% change in the variable factors used in calculating the ionization rates for the simulation shown in Fig. 7 resulted in noticeably poorer agreement between experiment and computer simulations of peak times and rates of increase in line intensities. The agreement shown in Fig. 7 is quite good, being poorest at late times when the rapid loss of plasma makes the computer simulation inaccurate. The overall accuracy of the ionization rates determined in this case is estimated to be about 30%, with about equal and independent contributions to the error from a remaining insensitivity of the fit, from electron density and temperature errors, and from ambiguities in the model.

The computer simulation of the plasma for case II using smoothed electron temperature and density histories is compared with the smoothed experimental time histories from Fig. 3 in Fig. 8. The peak electron temperature in case II is only about half that reached in case I, while the peak electron density in case II is almost five times higher than in case I. In this condition several time histories exhibit long tails of line radiation, while one, the Fe-X time history, actually levels off to a plateau for roughly 1 μsec before the plasma begins to decay.

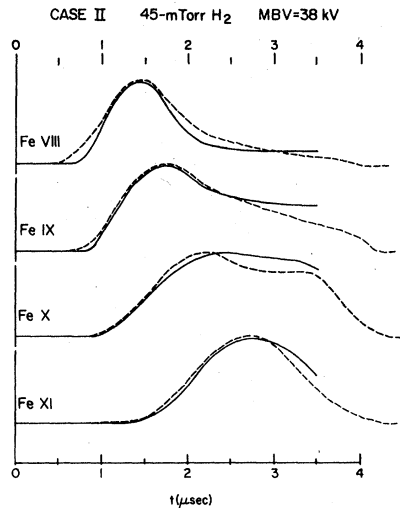It was impossible to duplicate even crudely

FIG. 8. Comparison of simulated (solid curves) and observed (dashed curves) time histories—case II (using zero-dimensional simulation and smoothed average values of T_e and n_e).

these features in the simulation when recombina- tion was neglected. Ionization-rate coefficients calculated from the semiempirical formula [Eq. (2)] were used, adjusted by the factors determined in case I. The calculations of Jacobs et al.[8] for the low-density limit of the dielectronic recombi- nation-rate coefficients were used as a first ap- proximation to the total effective recombination- rate coefficients. These were multiplied by factors which may be called "R_α," different for each ioni- zation stage, until the agreement shown in Fig. 8 was obtained. At an electron temperature of about 100 eV (case II) the recombination-rate coefficient determined in this way for Fe IX was 25% of its experimentally determined ionization-rate coeffi- cient, while that of Fe X was a factor of 2 greater than Fe X's ionization-rate coefficient. In the computer simulation the plateau in the Fe-X emis- sion resulted from a population equilibrium in the ground-state density of Fe X which lasted until the electron temperature began to drop.

Simulation of plasma cases I and II determined, therefore, both effective ionization- and recombi- nation-rate coefficients for these ions. For a check of the experimental procedure it was deemed desirable to simulate at least one other plasma condition in which the effect of recombination was evident in the line time histories. The combination of hydrogen-fill pressure and main bank voltage of case III was found to give a reproducible plasma condition in which the Fe-IX time history showed a distinct plateau, and the Fe-VIII time history a

long, sustained tail. As shown in Fig. 5, case III was found to have a peak average electron tempera- ture of only 65 eV, still lower than case II. Com- puter simulation using the experimentally deter- mined ionization- and recombination-rate coeffi- cients produced the agreement with the smoothed experimental time histories for case III shown in Fig. 9. The only free parameters used in obtaining this fit were the ionization-rate coefficients of Fe VI, VII, and VIII in the computer code. Because of the uncertainty at early times of the values of the rapidly changing temperature and density, these ionization rates were adjusted to cause the calculated Fe-VIII time history to peak at the ob- served time. All other ionization- and recombina- tion-rate coefficients remained as before, except for the application of the theoretical temperature scaling in going from the 200-eV value of case I to the 65-eV value of case III (ionization coefficients) or from 100 to 65 eV (recombination rates). The best-fit rate coefficients for these smoothed time histories were listed in Table I of Ref. 1.

The computer code used in the simulations lead- ing to the above results calculated the ionization, recombination, and excitation rates using the tem- perature and density values averaged over the ra- dius of the tube and smoothed to neglect the bounce mode oscillations which appear to be significant in cases II and III. In the detailed calculations de- scribed below, a one-dimensional computer code that takes into account the radial variation of elec- tron temperature and density was used.

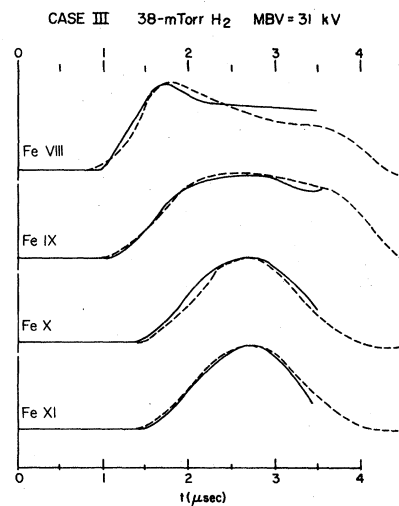These additional simulations were carried out

FIG. 9. Comparison of simulated (solid curves) and observed (dashed curves) time histories—case III (us- ing zero-dimensional simulation and smoothed average values of T_e and n_e).

realizing that the ion gyroradius is as large as the plasma radius[3,11] and as such, ionization and recombination take place throughout the plasma volume. Hence, average values of temperature and density are used in solving the coupled rate equations [Eq. (1)]. However, the actual measured radial profiles of the instantaneous electron temperature and density were used to calculate the time histories of the emission lines from Eq. (4) as the excitation process is a local phenomenon owing to the short radiative lifetimes. The intensity profiles computed at a number of points along the line of sight of the spectrometer were numerically integrated, using the Newton-Cotes rule, to yield the time histories that could be compared with experiment.

It was thus possible to find new values of the recombination factors R_α that more closely simulate the experimental time histories. Again, for ionization, the rates determined in case I were used taking temperature scaling into account as given by Eq. (2). Since the detailed radial profiles of electron temperature and density for case I correspond closely to the radial average used in the previous computation, there was no need to redo the calculations for this case.
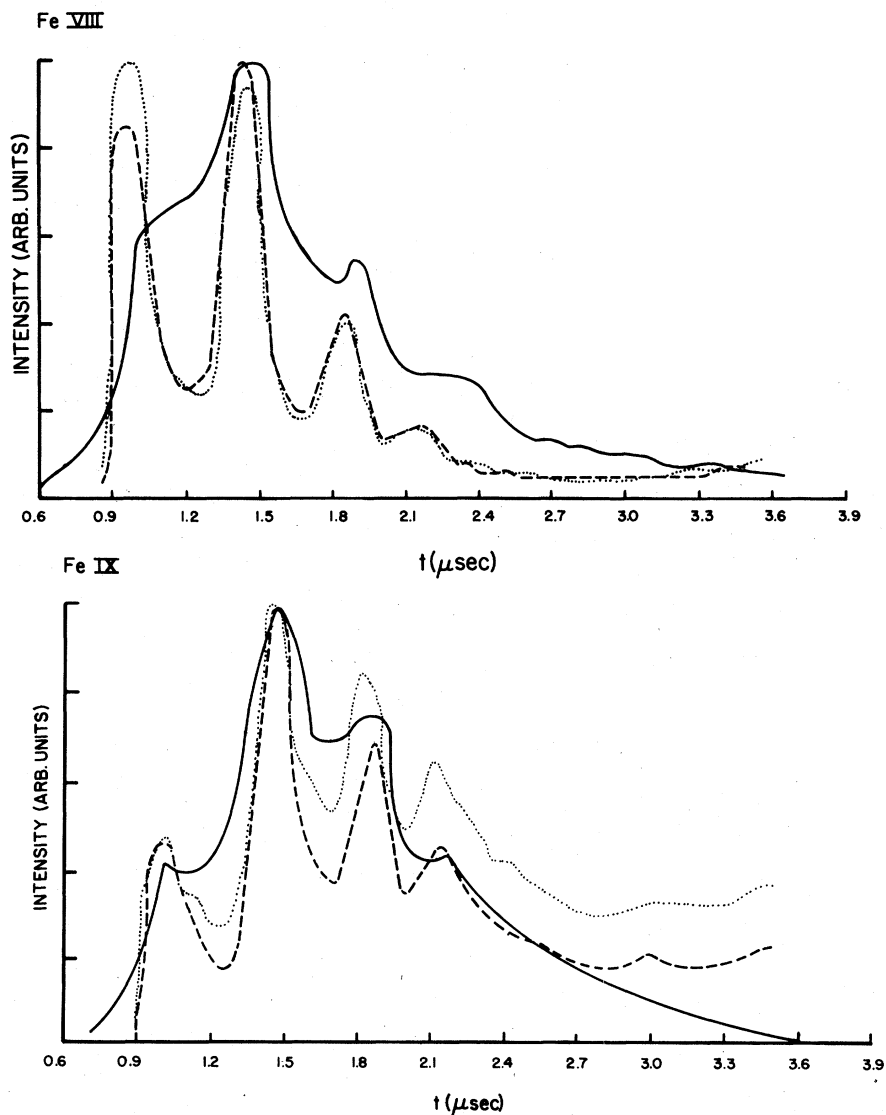

FIG. 10. Comparison of simulated (dashed curves) and observed (solid curves) time histories for case II using a one-dimensional simulation as described in the text. For the dashed curves the values of R_α used are those found to give the best fit with the one-dimensional simulation. The dotted curves were obtained using R_α values from the zero-dimensional simulation (corresponding to the values in parentheses in column 2 of Table II).
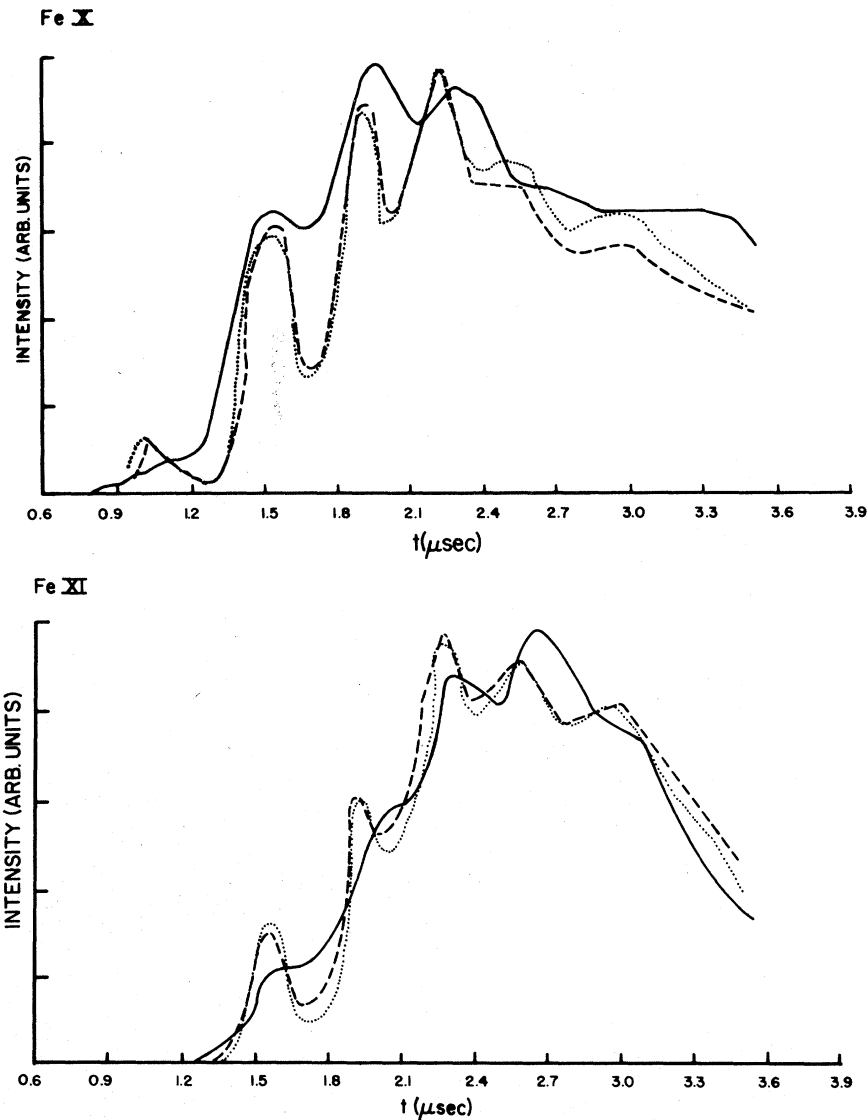
Fe X

Fe XI

FIG. 10 (Continued).

Figure 10 compares the computed time histories with the experimental time histories for case II using the best-fit values of R_α. These results are summarized in Table II and the best-fit values of R_α are given in column 2 for iron ions IX, X and XI. (R_α values obtained using radially averaged quantities are given in parentheses.)

For case III it was very difficult to make a direct comparison of the graphs for the computed and experimental time histories, as the low electron temperature for this case makes the excitation very sensitive to the actual value of T_e. The Thomson-scattering measurements on which the electron temperatures were based could not be made accurate enough to give a good comparison between computed and experimental emission line time histories at these low-plasma temperatures.

Several computations were run which included the effects of the temporal variation of plasma volume. These produced negligible differences in the results mentioned above. However, an attempt to solve the rate equations using the radial temperature and density oscillations at various points along the line of sight of the spectrometer did not yield time histories anywhere comparable to the experiment. This supports the correctness of the model employed in the detailed calculations.

V. CONCLUSIONS

As shown in Table II, the effective recombination rates at electron densities of $\sim 1-3 \times 10^{16}$ cm^3 are

TABLE II. Measured and calculated recombination (α) and ionization coefficients (S).

Ionization stage of Fe	$N_e = 1 - 3 \times 10^{16}$ cm^{-3} $T_e = 105$ eV	$N_e = 10^{10}$ cm^{-3} $T_e = 105$ eV	$T_e = 105$ eV	$T_e = 200$ eV	$T_e = 200$ eV
	a	b	c		d
	α_{expt}	α_{Jacobs}	S_{expt}	S_{expt}	S_{semi}
IX	2.4×10^{-10} (1.1)	2.7×10^{-10}			1.0×10^{-09}
X	0.9×10^{-10} (1.6)	2.3×10^{-10}	0.7×10^{-10}	3.2×10^{-10}	6.3×10^{-10}
XI	1.3×10^{-10} (2.2)	2.2×10^{-10}	0.4×10^{-10}	2.8×10^{-10}	4.0×10^{-10}
XII			0.3×10^{-10}	2.3×10^{-10}	2.3×10^{-10}

[a] Results using radially averaged temperatures and densities in parentheses (from Ref. 1).

[b] The calculated recombination coefficients, for $T_e = 105$ eV, are from Jacobs et al. (Ref. 8).

[c] The experimental ionization rates at $T_e = 105$ eV are derived from the experimental ionization coefficients at $T_e = 200$ eV by assuming the temperature dependence of Eq. (2).

[d] The semiempirical values of the ionization-rate coefficients at $T_e = 200$ eV are calculated as in Ref. 3.

nearly equal to or smaller than currently accepted theoretical dielectronic recombination rates for low-density plasmas. The ionization-rate coefficients also tend to be smaller than theoretical values.

The best-fit R_α values for Fe IX, Fe X, and Fe XI that result in the effective recombination rates shown in column 2 of Table II, are different for the various ions and models (zero or one dimensional). For each method, however, the R_α values obtained are internally consistent in that a 15% change in these factors is enough to produce disagreement between the simulated time histories and the experimentally observed ones. It is very difficult to ascertain the absolute error in the above results because of the possible systematic errors involved in making the comparisons.

An effort to find another combination of ionization- and recombination-rate coefficients which could duplicate the time histories of any of these three cases proved unsuccessful. The various plasma conditions are sensitive to one or both of the ionization- and recombination-rate coefficients, and good agreement was found between simulation and experiment in these three plasma conditions which exhibit widely varying parameters and iron line time histories. This argues strongly

for the reliability both of the computer simulation and of the experimentally determined coefficients. It also argues against the possibility of significant charge-exchange rates from hydrogen atoms.[12]

It is possible that the ionization rates used in case II had an additional uncertainty due to inaccuracy in the assumed temperature dependence from Eq. (2). Crossed-beam measurements of ionization cross sections for ions of carbon and nitrogen,[13] however, indicate that the temperature dependence of Eq. (2) should be accurate to within a factor of 2 over the temperature range of 50 to 250 eV.

We would be amiss not to point out that our effective recombination rates disagree with theoretical values calculated[14,15] for the actual (high) electron densities in our experiments. Such calculated values are smaller by about an order of magnitude, presumably because cross sections for electron collisions with ions in the contributing high Rydberg levels were overestimated in the calculations.

[1] R. L. Brooks, R. U. Datla, and Hans R. Griem, Phys. Rev. Lett. **41**, 107 (1978).

[2] C. Breton, C. De Michelis, M. Finkenthal, and M. Mattioli, Phys. Rev. Lett. **41**, 110 (1978).

[3] H. J. Kunze, Phys. Rev. A **3**, 937 (1971).

[4] R. U. Datla, L. J. Nugent, and H. R. Griem, Phys. Rev. A **14**, 979 (1976).

[5] E. S. Marmar, J. L. Cecchi, and S. A. Cohen, Rev.

Sci. Instrum. **46**, 1149 (1975).

[6] A. Sgro and C. Nielson, Phys. Fluids **19**, 126 (1976).

[7] H. J. Kunze, Space Sci. Rev. **13**, 565 (1972).

[8] V. L. Jacobs, J. Davis, P. C. Kepple, and M. Blaha, Astrophys. J. **211**, 605 (1977).

[9] M. J. Seaton, Mon. Not. R. Astron. Soc. **119**, 81 (1959).

[10] H. R. Griem, Plasma Spectroscopy (McGraw-Hill, New York, 1964), pp. 160–162.

[11]R. J. Commisso and H. R. Griem, Phys. Rev. Lett. <u>36</u>, 1038 (1976).

[12]R. C. Isler, Phys. Rev. Lett. <u>38</u>, 1359 (1977).

[13]D. H. Crandall, R. A. Phaneuf, B. E. Hasselquist, and D. C. Gregory, J. Phys. B <u>12</u>, L249 (1979).

[14]A. Burgess and H. P. Summers, Mon. Not. R. Astron. Soc. <u>174</u>, 345 (1976).

[15]V. L. Jacobs and J. Davis, Phys. Rev. A <u>18</u>, 697 (1978).